JOURNAL OF MATERIALS SCIENCE 25 (1990) 1563–1567

The interface microstructure in alumina (FP) fibre/magnesium alloy composite

M. PFEIFER
Department of Materials Science and Engineering, Northwestern University, Evanston, Illinois 60201, USA

J. M. RIGSBEE
Department of Materials Science and Engineering, University of Illinois at Urbana-Champaign, Illinois 61801, USA

K. K. CHAWLA*
Department of Materials and Metallurgical Engineering, New Mexico Institute of Mining and Technology, Socorro, New Mexico, 87801, USA

The objective of this work was to characterize the interfacial reaction zone in the metal matrix composite system α-Al_2O_3(FP)/Mg (ZE41A). The composite was fabricated by liquid infiltration method. The reaction zone, a result of the reaction between magnesium in the alloy and the alumina fibres, was analysed for its morphology, chemistry, and crystallographic orientation using transmission electron microscopy. The results of this study showed the reaction zone to be, on average, 100 nm wide and composed of MgO. The grains of the reaction zone ranged from less than 10 nm at the fibre/reaction zone interface to greater than 100 nm at the matrix/reaction zone interface. It is proposed that the growth of the reaction zone was controlled by a "seepage" mechanism involving infiltration of liquid magnesium between MgO crystals. Finally, it was observed that the MgO grains have the following crystallographic orientation relationship with the alumina grains from which they grew:

$$\langle 1\bar{1}0\rangle_{MgO} \parallel \langle 0110\rangle_{Al_2O_3} \quad \text{and} \quad \langle 111\rangle_{MgO} \parallel \langle 11\bar{2}0\rangle_{Al_2O_3}.$$

1. Introduction

It is of great importance to understand the structure and behaviour of the fibre/matrix interface, because this region controls the efficiency of load transfer. We have made a detailed characterization of the interface zone in the α-alumina(FP)/magnesium alloy (ZE41A) composite, because a reaction between the matrix magnesium alloy and the reinforcing alumina fibre during fabrication results in a reaction zone at the interface between the matrix and the fibre. It is well known that the presence of an interfacial reaction zone affects the mechanical properties of the bulk composite [1].

The reaction product in the system under study is magnesium oxide, and can be predicted from thermodynamics, oxidation potentials, and rates of reaction in an oxygen atmosphere, and has been shown to be so in several studies on this composite system [2–5]. However, other studies have also found, incorrectly, spinel [6, 7]. The present work further examines the morphology, chemistry, and orientation relationship with the fibre, of the interfacial reaction zone in the alumina (FP) fibre/magnesium alloy (ZE41A) composite system using transmission electron microscopy (TEM).

2. Material and experimental procedure

The metal matrix composite, α-Al_2O_3(FP)/Mg(ZE41A), had 35 vol% unidirectionally aligned fibres. The composite was fabricated by Du Pont Co. using liquid infiltration, a vacuum casting method in which the unidirectionally aligned fibres in a mould assembly were infiltrated with the molten magnesium alloy at 700 to 715° C.

The composition limits of the Mg ZE41A alloy are: Mg, 3.5% to 5.0% Zn, 0.4% to 1.0% Zr, 0.75% to 1.75% rare earth metals (as mischmetal), 0.15% Mn (maximum), 0.10% Cu (maximum), 0.01% Ni (maximum), and 0.30% others (maximum) [8]. The alumina fibre, Du Pont's FP fibre, is > 99% α-Al_2O_3, continuous, polycrystalline fibre about 20 μm diameter.

As-cast samples of the Al_2O_3/Mg(ZE41A) composite were used to study and analyse the reaction zone formed between the matrix and fibre. The as-cast specimens were analysed using transmission electron microscopy with Philips EM400T, EM420T, and EM430T electron microscopes. TEM samples were prepared by first slicing thin foils from the bulk samples and mechanically polishing these to a thickness of 90 μm. TEM samples, 3 mm thick, were then mechanically punched out from the thinned foils, using a

Present address: Division of Materials Research, National Science Foundation, Washington, DC 20550, USA.

0022–2461/90 $03.00 + .12

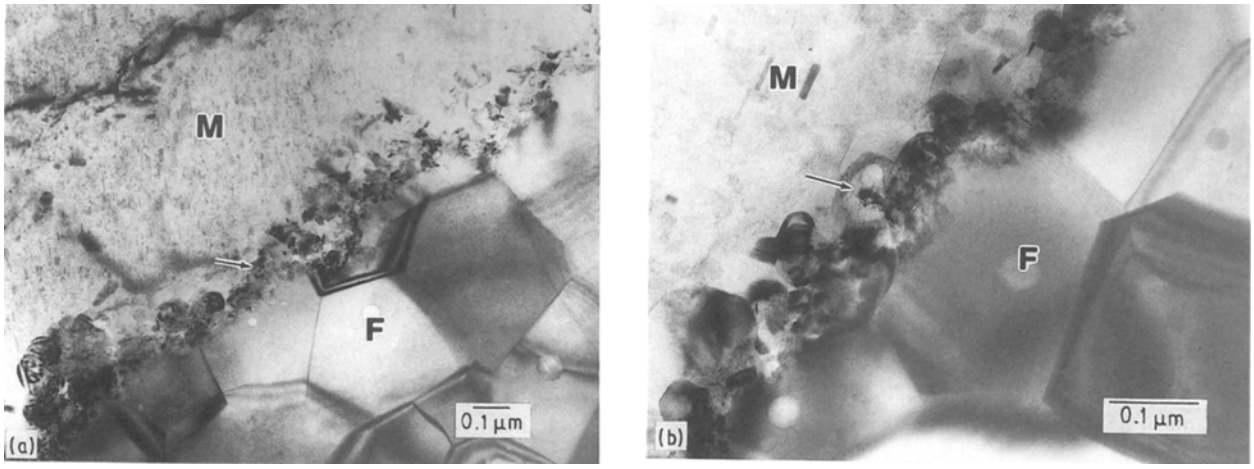

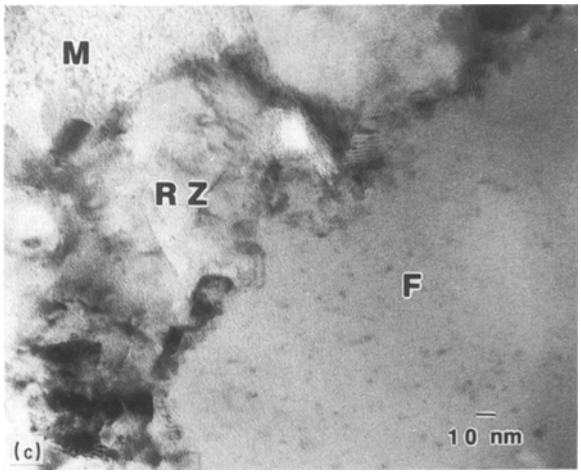

Figure 1 (a) Bright-field image of the reaction zone (arrow) and the surrounding matrix (M) and fibre (F). (b) High magnification bright-field image of the reaction zone region. (c) Same as (a), but at a higher magnification.

punch and die assembly, mechanically thinned to 25 μm, and finally ion milled to electron transparency.

3. Results

3.1. Morphology of the reaction zone

The fibre (F), the matrix (M) and the reaction zone (rz), (arrow) are shown in Fig. 1a. There are two interfaces: the fibre/reaction zone and the reaction zone/matrix. The average width of the reaction zone is about 0.1 μm. Note that a portion of each alumina grain on the outside edge of the fibre has been consumed in the reaction between the molten alloy and the fibre during fabrication. In a higher magnification of a different reaction zone area, Fig. 1b, many of the smaller reaction zone grains at the fibre/reaction zone interface are outlined with Moiré fringes, making it easier to distinguish their size and shape. The overall morphology of the reaction zone is also clearer here, where the oblong-shaped reaction zone grains are seen to range in size from less than 10 nm at the fibre/reaction zone interface, increasing across the width of the reaction zone, to greater than 0.1 μm at the matrix/reaction zone interface, better indicated in Fig. 1c. Finally, the jagged nature of the fibre/reaction zone interface is apparent, further indicating that the alumina fibre has been consumed in the reaction between the matrix and the fibre.

3.2. Composition of the reaction zone

It was necessary to use selected-area diffraction (SAD) and microdiffraction of the reaction zone grains in order to determine the reaction product. SAD was used on the larger grains closer to or at the reaction zone/matrix interface and over the whole width of the reaction zone, while microdiffraction was used on the smaller grains. Results of these diffraction analyses are shown in Fig. 2. The electron diffraction spot patterns were obtained using either SAD or microdiffraction of the larger reaction zone grains; whereas the spotty electron diffraction ring patterns (Fig. 2c) were obtained by using SAD of the smaller reaction zone grains closer to the fibre/reaction zone interface. The diffraction rings, a result of diffraction by many small reaction zone grains, are spotty because the smallest SAD aperture had to be used, the others being wider than the reaction zone, leading to incomplete rings as a result of not having enough grains to contribute to the diffraction pattern.

Because of the materials involved in the reaction it was initially assumed that the reaction zone would be composed of MgO. This was proved to be true, as all the diffraction patterns could be easily analysed according to the parameters defined by the MgO crystallography. The diffraction patterns in Fig. 3 are thus indexed accordingly.

3.3. Crystallography of the reaction zone

Using microdiffraction and SAD it was possible to determine orientation relationships between the reaction zone and the alumina grain from which it grew. These relationships are

$$\langle 1\,\bar{1}\,0\rangle_{MgO} \parallel \langle 0\,1\,1\,0\rangle_{Al_2O_3}$$

$$\langle 1\,\bar{1}\,1\rangle_{MgO} \parallel \langle 1\,1\,\bar{2}\,0\rangle_{Al_2O_3}$$

and hold for all conditions in the as-received composite, except for the very large MgO grains, greater than about 80 nm, sticking into the matrix from the reaction zone.

This relationship is partially shown in Fig. 3 where the $[1\,\bar{1}\,0]_{MgO}$ zone axis SAD pattern is parallel to the $[\bar{1}\,1\,0\,0]$ Al_2O_3 zone axis SAD pattern, obtained without specimen tilt between the two zone axes diffraction patterns. The bright-field image, Fig. 4, under these

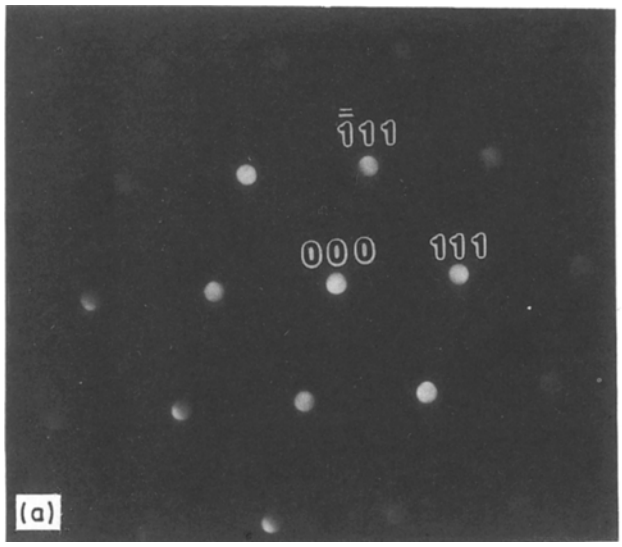

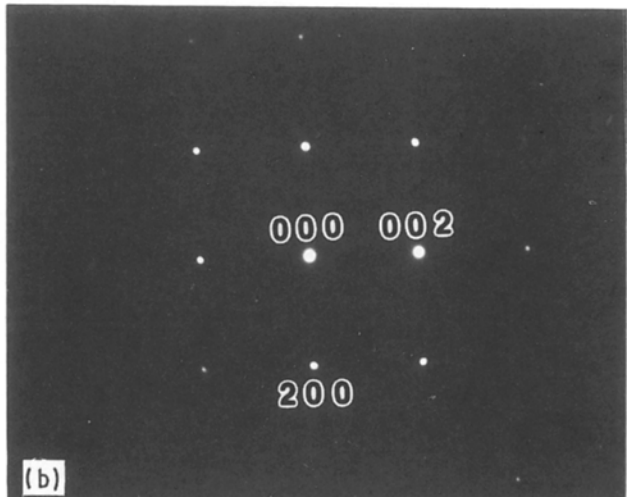

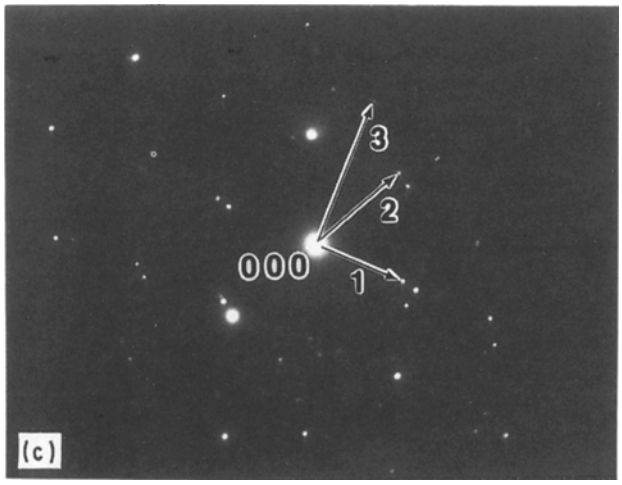

Figure 2 (a) Microdiffraction pattern of an MgO grain, $\boldsymbol{B} = z = [0\,1\,1]$. (b) SAD pattern of an MgO grain, $\boldsymbol{B} = z = [0\,1\,0]$. (c) SAD pattern showing partial ring pattern for MgO.

conditions shows the reaction zone and the corresponding alumina grain diffracting strongly as several planes in each crystal system are satisfying diffraction conditions at this specimen tilt. The dark-field image, Fig. 5, obtained by using a simultaneous MgO/Al_2O_3 two-beam condition (inset) in which an MgO diffracted spot lay adjacent to an Al_2O_3 diffracted spot, has the alumina grain and many of the reaction zone MgO grains strongly diffracting, but no contribution from the matrix. This image also indicates that the orientation relationship between the reaction zone grains and each alumina grain has variants of the relationship $\langle 1\,1\,0\rangle_{MgO} \parallel \langle 1\,0\,\bar{1}\,0\rangle_{Al_2O_3}$, because many of the MgO grains are not diffracting at the specific diffraction conditions of this image. If the sample were to be tilted to other $\langle 1\,0\,\bar{1}\,0\rangle$ Al_2O_3 orientations, different MgO grains would be seen to be strongly diffracting.

As for the very large MgO grains, greater than about 80 nm diameter, sticking out from the reaction zone into the matrix, no orientation relationship was found with respect to alumina grains on which they had originally grown. This is illustrated in Fig. 6 which is a bright-field image using $\boldsymbol{g} = [0\,\bar{1}\,1]$. As none of the rest of the reaction zone is even slightly diffracting, this particular grain fails the orientation relationships already established.

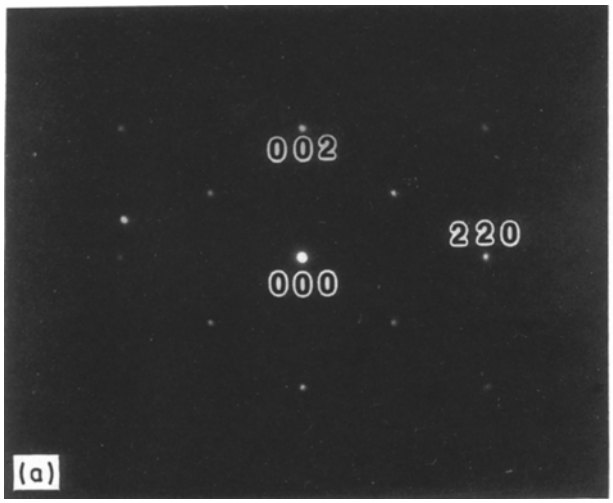

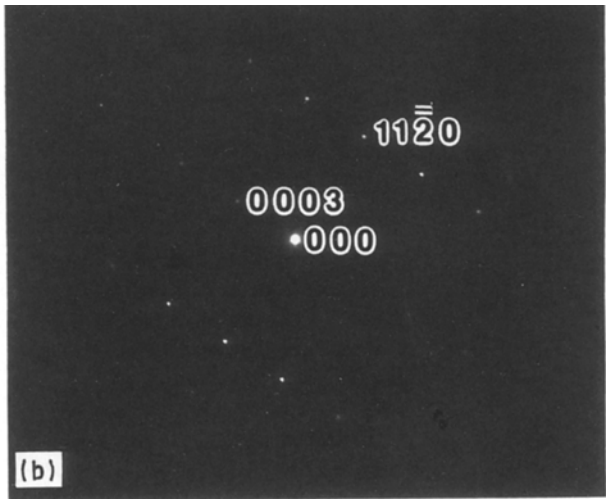

Figure 3 Parallel zone axis patterns of an MgO grain and the Al_2O_3 grain from which it grew. (a) MgO, $\boldsymbol{B} = z = [1\,1\,0]$; (b) Al_2O_3, $\boldsymbol{B} = z = [1\,1\,0\,0]$.

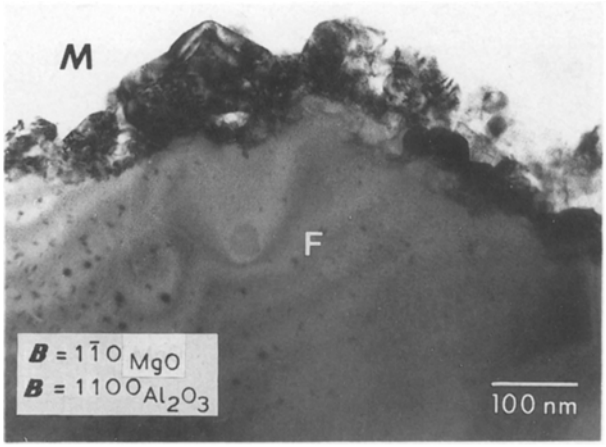

Figure 4 Bright-field image using the conditions shown in Fig. 3.

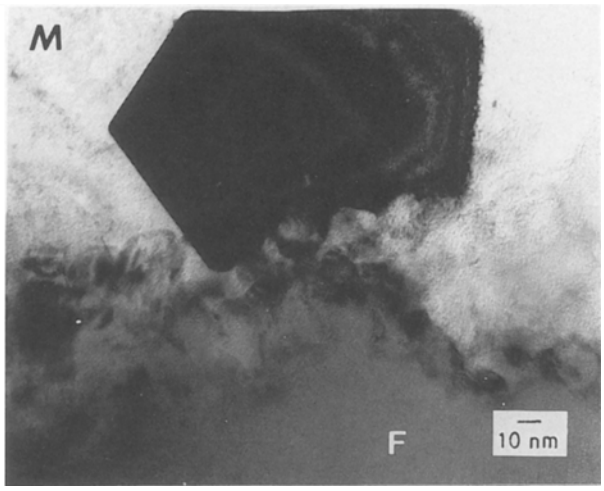

Figure 6 Bright-field image of a strongly diffracting MgO reaction zone grain. $\boldsymbol{B} = z = [0\,\bar{1}\,1]$ with respect to this grain.

4. Discussion

When the evacuated mould containing the unidirectional fibres is first infiltrated with the molten magnesium, a reaction at the alumina fibre/liquid magnesium alloy interface takes place according to

$$Al_2O_3(s) + 3Mg(l) \rightarrow 3MgO(s) + 2Al(l)$$

This reaction is expected to proceed in the direction indicated for three reasons: (1) the oxidation potential for magnesium is greater than that for aluminium; (2) this reaction results in a lowering of the free energy of the system; (3) the ability for magnesium to form its oxide is about 10^8 times higher than that of aluminium at any temperature [9]. Furthermore, these results are the most favourable considering the different elements in the alloy (magnesium, zinc, zirconium). Thus, the whole reaction zone should consist of MgO, as has been shown in the results above.

This, of course, correlates with earlier results [2–5]. However, fine precipitates of the spinel $MgO–Al_2O_3$, in addition to MgO, were observed by some researchers [6, 7]. No such reaction product was detected in the present case. The phase diagram for the $MgO–Al_2O_3$ system [10] only goes down to about 1100° C; it is difficult to say whether the spinel should form during fabrication of the composite. But, it appears that with extrapolation of the boundaries for the spinel region of the phase diagram down to 715° C there would be no spinel formation, except perhaps at extended periods of time at this temperature.

From the morphology of the reaction zone it is also possible to discuss the kinetics of this reaction, a solid(1) + liquid → solid(2) reaction, where the liquid magnesium reacts with the solid alumina and immediately forms solid MgO. This results because the molten magnesium alloy, when the mould is initially infiltrated, is at 700 to 715° C, whereas the melting point of MgO is 2852° C.

From the size distribution of the MgO grains, going across the width of the reaction zone, it appears that the MgO grains closer to the matrix/reaction zone interface had more time to grow than those closer to the reaction zone/fibre interface. This is explained by the following mechanism of nucleation and growth of the reaction zone that we propose. The reaction zone nucleation starts as the liquid magnesium first comes in contact with the alumina fibre grains. The MgO grains nucleate and grow on the edges of the alumina grains, where only the alumina originally existed. MgO grain nucleation occurs further into the original alumina grain as the molten magnesium alloy seeps in between already nucleated, and growing, MgO grains, and reacts with the alumina at the pre-existing reaction zone/alumina interface. This seepage process during infiltration continues until the MgO grains closer to the matrix/reaction zone interface have grown large enough to close off the spaces between these grains, stopping the seepage, or until the magnesium alloy is fully solid.

This correlates with the morphology of the reaction

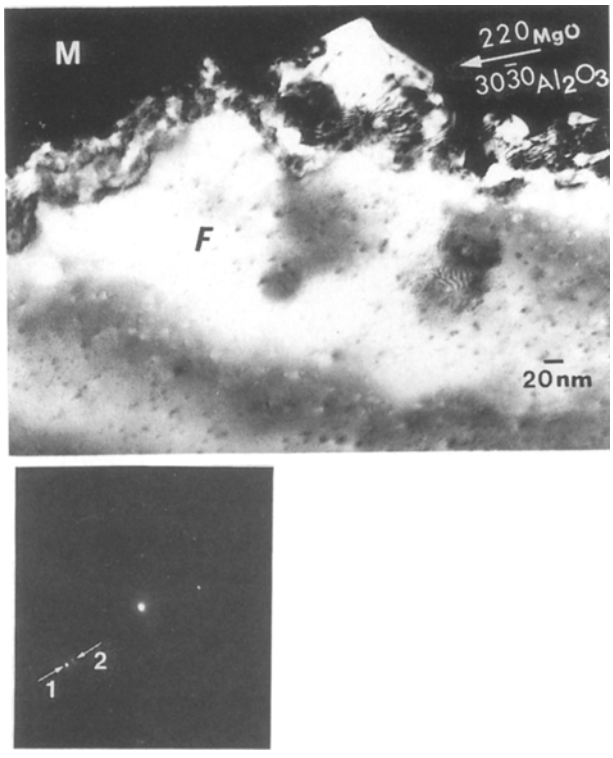

Figure 5 Dark-field image using the simultaneous z-beam condition shown in the inset with: $1\boldsymbol{g} = [\bar{3}\,0\,3\,0]_{Al_2O_3}$; $2\boldsymbol{g} = [2\,2\,0]_{MgO}$.

zone as the MgO grain size increases with distance from the reaction zone/fibre interface. The small MgO grains closer to the reaction zone/fibre interface did not have as much time to grow as those closer to the matrix/reaction zone interface, the seepage mechanism having been shut off by the larger grains closer to the matrix/reaction zone interface.

There is still the question of continued growth of the MgO grains at the matrix/reaction zone interface, as there are no alumina grains in the immediate vicinity with which to react. In this case it should be observed that the magnesium in the molten alloy would react with oxygen present in the mould according to

$$2Mg(l) + O_2 \rightarrow 2MgO(s)$$

This reaction probably occurs throughout the matrix, with the reaction zone MgO grains growing as the reaction proceeds at the matrix/reaction zone interface, the newly formed MgO growing on to the reaction zone grains. Because the equilibrium partial pressure of oxygen for this reaction is 10^{-50} atm it would easily go to the right even during the vacuum infiltration process used [11].

Furthermore, from the limited diffusion data that exist (from 1400° C to 1600° C), the diffusivity of magnesium through MgO [11] would be too low at fabrication temperatures to have diffusion of magnesium through the MgO, forming more MgO on the pre-existing reaction zone grains at the reaction zone/alumina fibre interface. Finally, as shown, all but the MgO reaction zone grains larger than about 80 nm, show orientation relationships with the alumina fibre grain from which they grew. The failure of the very large reaction zone grains at the matrix/reaction zone interface to follow the orientation relationships described is probably a result of these grains being pushed and tilted around by the MgO grains growing further from the matrix/reaction zone interface.

5. Conclusions

The reaction zone between the metal matrix and ceramic fibres in the α-Al_2O_3(FP)/Mg(ZE41A) composite system was analysed. The conclusions based on morphological, chemical, and crystallographic analyses are as follows.

1. The reaction zone is, on average, 100 nm wide, and is comprised of grains ranging from less than 10 nm at the reaction zone/fibre interface and increasing across the width of the reaction zone/fibre to greater than 100 nm at the matrix/reaction zone interface.

2. The reaction zone formed by the reaction

$$3Mg(l) + Al_2O_3(s) \rightarrow 3MgO(s) + 2Al(l)$$

3. The extent of the above reaction was limited by the kinetics of the reaction. A "seepage" mechanism involving infiltration of liquid magnesium between MgO crystals could be the controlling mechanism. When MgO grains closer to the matrix/reaction zone interface grew large enough to close off cracks leading toward the reaction zone/fibre interface, the reaction given above ceased.

4. The crystallographic orientation relationships between the reaction zone grains and the alumina grains from which they grew, are

$$\langle 1\,1\,0\rangle_{MgO} \parallel \langle 0\,1\,\bar{1}\,0\rangle_{Al_2O_3}$$

$$\langle 1\,1\,1\rangle_{MgO} \parallel \langle 1\,1\,\bar{2}\,0\rangle_{Al_2O_3}$$

These relationships hold for all but the very large reaction zone grains at the matrix/reaction zone interface.

Acknowledgement

We thank Du Pont Co. for providing the composite samples.

References

1. K. K. CHAWLA, "Composite Materials: Science and Engineering" (Springer Verlag, New York, 1987).
2. J. E. HACK, R. A. PAGE and R. SHERMAN, *Met. Trans.* **16A** (1985) 2069.
3. R. A. PAGE, J. E. HACK, R. SHERMAN and G. R. LEVERANT, *ibid.* **15A** (1984) 1397.
4. C. G. LEVI, G. J. ABBASCHIAN and R. MEHRABIAN, *ibid.* **9A** (1978) 697.
5. C. S. LEE, K. K. CHAWLA, J. M. RIGSBEE and M. PFEIFER, in "Cast Reinforced Metal Composites", (American Society for Metals, Metals Park, Ohio, 1988) p. 301.
6. J. NUNES, E. S. C. CHIN, J. M. SLEPETZ and N. ISANGARAKIS, in the International Conference on Composite Materials, ICCM-V, Conference Proceedings (Pergamon, Oxford, 1985) p. 723.
7. E. S. C. CHIN, MS thesis, Brown University, Providence, Rhode Island (1983).
8. "Metals Handbook" 9th edition, Vol. 2, "Properties and Selection: Nonferrous Alloys and Pure Alloys", (ASM Metals Park, Ohio, 1987) p. 591.
9. D. R. GASKELL, "Introduction to Metallurgical Thermodynamics", (Hemisphere, New York, 1981) p. 287.
10. W. D. KINGERY, H. K. BOWEN and D. R. UHLMANN, "Introduction to Ceramics", (Wiley, New York, 1976) p. 133.
11. R. LINDER and G. D. PARFITT, *J. Chem. Phys.* **26** (1957) 182.

Received 10 January
and accepted 16 August 1989